Eur. J. Mineral.
2001, **13**, 1177-1190

# Shock-related mineralogical features and P-T history of the Suizhou L6 chondrite

XIANDE XIE*, MING CHEN and DEQIANG WANG

Guangzhou Institute of Geochemistry, Chinese Academy of Sciences
510640 Guangzhou, P.R. China

**Abstract:** The Suizhou meteorite, classified as an L6 chondrite, contains weakly shocked olivine and pyroxene, but almost all the plagioclase in the meteorite was melted and transformed into maskelynite during shock metamorphism. Chromite was heavily fragmented and granulated, and many tiny chromite fragments were incorporated into the molten plagioclase as inclusions. Metal and troilite show no obvious intragranular textures, but many tiny rounded FeNi metal grains were deposited in the intersecting joints of planar fractures in olivine and pyroxene. A few very thin shock melt veins occur in the Suizhou meteorite, which contain abundant high-pressure phases, including coarse-grained ringwoodite, majorite, (Na,Ca)$AlSi_3O_8$-hollandite and fine-grained liquidus majorite-pyrope garnet. The shock features of this meteorite match shock stages 3 to 5, while the presence of ringwoodite in Suizhou veins is considered to appear at stage 6. It is estimated that the Suizhou meteorite experienced a shock pressure and shock temperature of up to 22 GPa and 1000°C, respectively. The shearing friction along veins raised the temperature within the veins. Shock-induced pressure and temperature in the shock veins attained 22 GPa and 1900°C. Therefore, the actual shock level of the Suizhou meteorite could correspond to stage 3-4. A longer duration of the shock pressure and temperature regime in the Suizhou meteorite plays an important role in the pervasive melting of plagioclase in the unmelted part of the meteorite, as well as in the formation of abundant high-pressure phases in the very thin shock-melt veins. It appears that maskelynite cannot be used as the sole criteria for evaluating the shock stage of shock-metamorphosed chondrites.

**Key-words:** Shock vein, high-pressure phase, maskelynite, P-T history, Suizhou meteorite.

## 1. Introduction

Shock-induced deformation features are observed in many chondritic meteorites (Fredriksson *et al.*, 1963; Carter *et al.*, 1968; Binns *et al.*, 1969; Ashworth & Barber, 1975, 1976; Dodd & Jarosewich, 1979; Stöffler *et al.*, 1988, 1991; Chen *et al.*, 1995, 1996, 2000; Xie *et al.*, 1991, 2000a, 2000b, 2001). Detailed studies on these phenomena were carried out in an attempt to quantify these features in terms of progressive stages of shock metamorphism and estimate the peak shock pressures and temperatures (Stöffler *et al.*, 1991; Schmitt & Stöffler, 1995). Stöffler *et al.* (1991) defined a scheme of six stages of shock (S1 to S6) on the basis of shock effects in olivine and plagioclase, and proposed a shock-pressure calibration for these stages on the basis of a critical evaluation of data from shock recovery experiments. These authors also reported that shock melt veins are not critical for the definition of the shock stage even though their presence indicates that the meteorite is shocked to stage 3 or above (Stöffler *et al.*, 1991). Their scheme (Stöffler *et al.*, 1991) reveals a progressive increase in the abundance of opaque shock veins (S3), ranging from melt pockets, inter-

*e-mail: xdxie@gis.sti.gd.cn

DOI: 10.1127/0935-1221/2001/0013-1177 0935-1221/01/0013-1177 $ 3.50

connecting melt veins and opaque shock veins (S4) to the pervasive formation of melt pockets, melt veins and opaque shock veins (S5 and S6). Diaplectic plagioclase glass ("maskelynite") appears in stage S5, whereas the high-pressure polymorph of olivine, ringwoodite, is seen in restricted local domains at stage S6. The shock-pressure range for the reconstructive olivine – ringwoodite transition is thought to be between 45 and 90 GPa and the post shock temperature between 600°C and 1750°C (Stöffler *et al.*, 1991).

The Suizhou meteorite is a shock-vein-bearing L6 chondrite. The shock features of the Suizhou meteorite match shock stages from 3 to 6 of the scheme defined by Stöffler *et al.* (1991), and cover a wide range of high pressures from 5 to > 45 GPa. In this paper, we describe the shock-related mineralogical features of the Suizhou meteorite and try to draw some conclusions on the *P-T* history of this meteorite.

## 2. Methods of study

The petrographic features were observed from the hand specimen of the Suizhou meteorite. Two fragments of the meteorite, one containing melt veins, were made into polished thin sections (PTS). The mineralogical features and the texture of rock were investigated on PTS using a MPV-SP optical microscope (OM) and a Hitachi S-3500N scanning electron microscope (SEM) at the Guangzhou Institute of Geochemistry, Chinese Academy of Sciences. Chemical compositions of mineral phases were analysed using a Cameca SX-51 electron microprobe (EMPA) at 15 kV and 10 nA at the Institute of Geology, Chinese Academy of Sciences. Raman spectra of both low-pressure and high-pressure phases were recorded on a Renishaw RM-1000 laser Raman microscope ($Ar^+$ laser, 514.5-nm line) in the Beijing Institute of Non-Ferrous Metals.

## 3. Results

### 3.1 General features of the shock-metamorphosed Suizhou meteorite

The Suizhou meteorite fell on April 15, 1986, at Dayanpo, which is located 12.5 km to the southeast of Suizhou city, Hubei Province, China. A total weight of 270 kg of this meteorite has been collected, and the largest piece, a fragment of 56 kg in weight, is now preserved in the City Museum of Suizhou. This meteorite was classified as an L6 chondrite, and was evaluated by previous investigators (Wang & Li, 1990; Wang, 1993) as a weakly shock-metamorphosed (S2 to S3) meteorite.

The determination of the cosmogenic nuclides $^{3}He$, $^{21}Ne$, $^{35}Ar$, $^{83}Kr$ and $^{126}Xe$, as well as the $^{81}Kr$-Kr dating, indicate that the Suizhou meteorite has an average cosmic-ray exposure age of 29.8 ± 3.5 Ma (Wang, 1993). The results obtained by different methods are in good agreement within the limits of experimental errors, hence indicating that the meteorite has only a single-stage cosmic-ray exposure history. The parent body of the meteorite broke up as a result of a collision to form the Suizhou meteorite at about 30 Ma ago (Wang, 1993).

K-$^{40}Ar$ dating of the Suizhou meteorite yielded an age of 4280 Ma, clearly younger than its formation age (4580 Ma). This indicates radiogenic $^{40}Ar$ losses after the formation of the meteorite, but no loss of the cosmogenic nuclide $^{3}He$ since exposure of the Suizhou meteorite to cosmic rays soon after its separation from the parent body (Wang, 1993). Therefore, the loss of radiogenic $^{40}Ar$ took place before the formation of the Suizhou meteorite and has no relation with the later shock event. This implies that the Suizhou meteorite was weakly shocked (S3) and the shock pressure should be below 10 GPa (Stöffler *et al.*, 1991).

The fresh fragment surface of the Suizhou meteorite has a light-grey colour. The meteorite consists of olivine, low-Ca pyroxene, plagioclase, kamacite, taenite, troilite, chromite and whitlockite. Our recent studies of the Suizhou meteorite indicate that abundant irregular and planar fractures were developed in olivine and pyroxene, and almost all the plagioclase was melted (Fig. 1 and 2). Shock melt veins are very poorly developed in the meteorite and only a few very thin melt veins are observed ranging from 20 to 90 μm in width (Fig. 1). These veins usually extend in only one direction and there are no networks of veins. The boundaries separating the black vein material from the light-coloured unmelted chondritic rock are sharp and straight. The shock veins are mainly composed of fine-grained matrix that makes up 80~90 volume % of the veins. Our microprobe and Raman spectroscopic investigations shaw that the matrix material consists of idiomorphic granular majorite-pyrope garnet, irregular Fe-Ni metal and troilite grains in eutectic intergrowths, while the remaining 10~20 volume % of veins consist of coarse-grained high-pressure polymorphs of

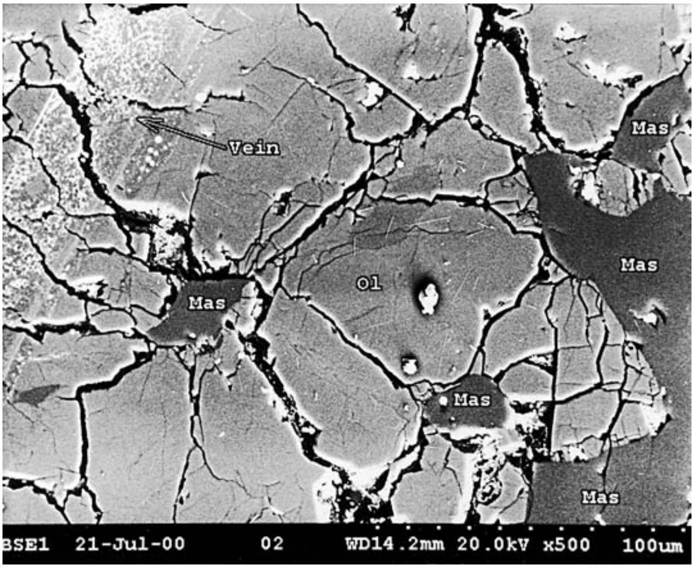


Fig. 1. Back-scattered electron (BSE) image showing maskelynite (Mas) surrounded by radiating cracks in neighbouring olivine (Ol) and pyroxene in the Suizhou unmelted chondritic rock. A thin shock-melt vein (Vein) intersects the chondritic rock (upper-left part of the image).

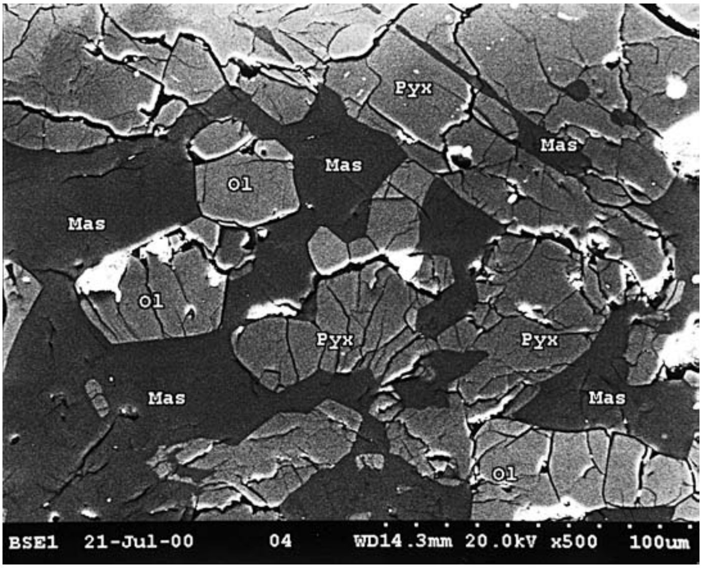


Fig. 2. BSE image showing irregular and planar fractures in olivine (Ol) and pyroxene (Pyx), and maskelynite (Mas) with flow-deformed shape filling open cracks and fractures in olivine and pyroxene.

silicate minerals (Xie *et al.*, 2000a, 2000b). "Shock blackening" effect and shock-induced melt pockets were not encountered in the Suizhou meteorite.

### 3.2 Weakly-shocked olivine and pyroxene

Olivine is the most abundant constituent mineral (~ 60 % by volume) in the unmelted domain of

Table 1. Compositions of minerals in the Suizhou meteorite (wt %)

| | Rgt | Ol | Mjt | Pyx | Mj-Py |
|---|---|---|---|---|---|
| No | 4 | 3 | 6 | 2 | 3 |
| $SiO_2$ | 38.39 | 38.25 | 55.82 | 55.78 | 50.53 |
| $TiO_2$ | 0.02 | 0.02 | 0.18 | 0.18 | 0.12 |
| $Al_2O_3$ | 0.01 | 0.00 | 0.16 | 0.16 | 3.51 |
| FeO | 23.26 | 22.35 | 14.27 | 13.95 | 13.61 |
| MnO | 0.40 | 0.48 | 0.51 | 0.48 | 0.36 |
| MgO | 38.69 | 39.18 | 28.97 | 29.31 | 28.13 |
| CaO | 0.05 | 0.01 | 0.72 | 0.70 | 1.92 |
| $Na_2O$ | 0.00 | 0.01 | 0.10 | 0.03 | 0.87 |
| $K_2O$ | 0.01 | 0.01 | 0.02 | 0.01 | 0.05 |
| $Cr_2O_3$ | 0.04 | 0.03 | 0.12 | 0.10 | 0.39 |
| NiO | 0.04 | 0.04 | 0.06 | 0.01 | 0.24 |
| Totals | 100.91 | 100.38 | 100.93 | 100.71 | 99.73 |
| | | | Number of cations | | |
| Si | 1.00 | 1.00 | 0.99 | 0.99 | 3.60 |
| Ti | 0.00 | 0.00 | 0.00 | 0.00 | 0.00 |
| Al | 0.00 | 0.00 | 0.01 | 0.01 | 0.30 |
| Fe | 0.50 | 0.49 | 0.22 | 0.21 | 0.80 |
| Mn | 0.01 | 0.01 | 0.01 | 0.01 | 0.02 |
| Mg | 1.49 | 1.50 | 0.77 | 0.79 | 3.04 |
| Ca | 0.00 | 0.00 | 0.02 | 0.02 | 0.18 |
| Na | 0.00 | 0.00 | 0.00 | 0.00 | 0.22 |
| K | 0.00 | 0.00 | 0.00 | 0.00 | 0.00 |
| Cr | 0.00 | 0.00 | 0.00 | 0.00 | 0.02 |
| Ni | 0.00 | 0.00 | 0.00 | 0.00 | 0.00 |
| Totals | 2.00 | 2.00 | 2.02 | 2.02 | 8.18 |
| Oxygen | 4 | 4 | 3 | 3 | 12 |

Rgt, ringwoodite; Ol, olivine; Mjt, majorite; Pyx, pyroxene; Mj-Py, majorite-pyrope garnet; No, number of analysis.

the Suizhou meteorite. This mineral displays wavy extinction, irregular fractures and from one to four sets of parallel planar fractures with a spacing of tens of micrometers (Fig. 2). It has a grain size ranging from 0.05 mm to 0.5 mm. In some parts of the thin sections, the olivine grains are granulated with a grain size of less than 0.01 mm, but we observed no mosaic-like or planar deformation features (PDF), or solid state recrystallization in olivine. Microprobe analyses show that the olivine has the composition of $(Mg_{1.50}Fe_{0.49}Mn_{0.01})_2SiO_4$ (Table 1). Raman spectra recorded from olivine grains show strong and sharp peaks at 821 and 851 $cm^{-1}$ (Fig. 3a) that are characteristic of a low-pressure phase of olivine.

Low-calcium pyroxene in the Suizhou meteorite displays wavy extinction, irregular fractures (Fig. 2) and mechanical polysynthetic twinning, with a grain size of 0.05–0.8 mm. Shock-induced granulation (down to grain sizes of < 0.02 mm) is also observed in some grains, but no PDF, mosaic structures or transformation into molten state were found in the Suizhou pyroxene. Microprobe study shows that low-calcium pyroxene has the composition $(Mg_{0.79}Fe_{0.21}Ca_{0.02})_{1.02}(Si_{0.99}Al_{0.01})_{1.00}O_3$ (Table 1). Raman analyses display sharp peaks at 390, 664 and 1011 $cm^{-1}$ (Fig. 3b), indicating that this is a low-pressure phase of pyroxene.

From the above description, it is clear that both olivine and pyroxene in the Suizhou chondrite were only shocked to stage 3 according to the clsification of Stöffler *et al.* (1991).

### 3.3 Strongly-shocked and melted plagioclase

Plagioclase is a common rock-forming mineral in L-group chondrites. However, we found that almost all plagioclases in the Suizhou meteorite were melted and transformed into maskelynite. The maskelynite, representing a quenched high-pressure melt, contains no cleavages and scarce fractures, and displays a smooth

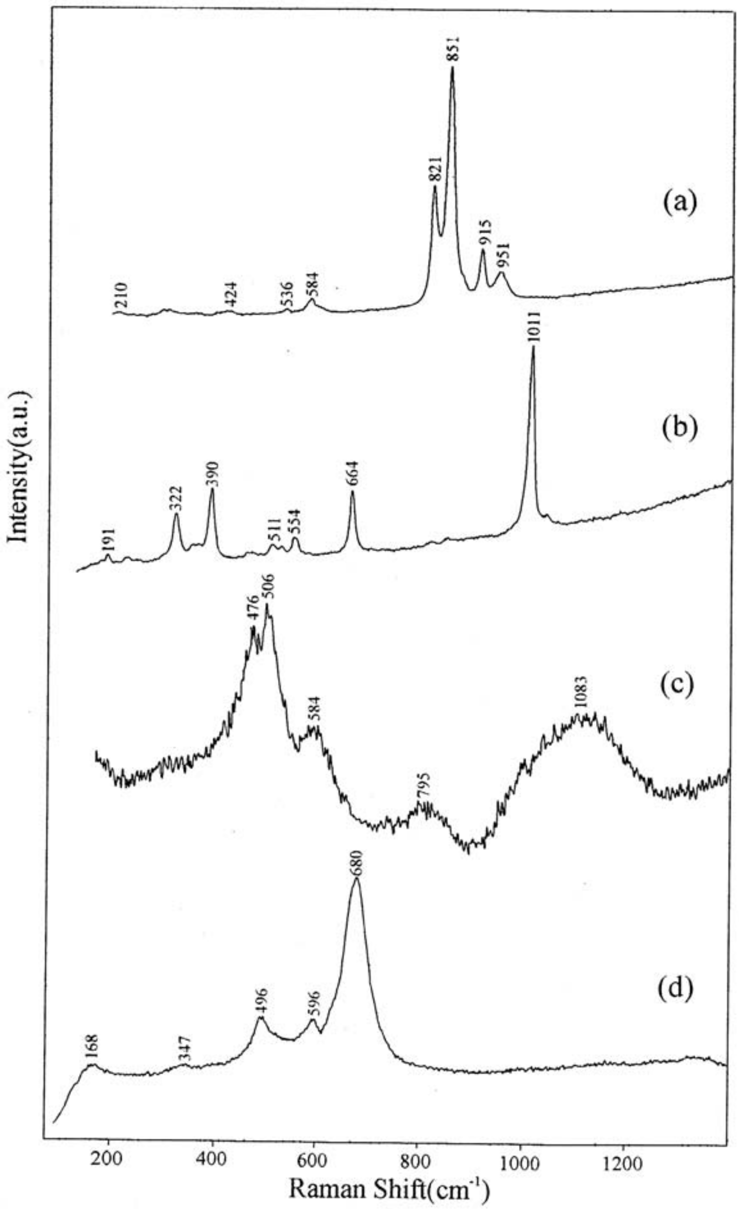


Fig. 3. Raman spectra of minerals in the Suizhou unmelted chondritic rock. (a) olivine, (b) pyroxene, (c) molten plagioclase, and (d) chromite.

surface (Fig. 1 and 2). Under the optical microscope, it shows isotropic properties. Some maskelynite grains contain abundant tiny fragments of chromite (Fig. 4 and 5), or olivine and pyroxene (Fig. 2 and 4). Raman spectroscopic investigations of maskelynite display several broad bands in the ranges of 950–1250, 760–840, and 400–650 $cm^{-1}$ (Fig. 3c). Only a few small grains of untransformed plagioclase are observed in thin sections.

Maskelynite grains are usually surrounded by radiating cracks which penetrate deeply into the neighbouring olivine and pyroxene as a result of volume expansion from the original crystal phase to melt glass (Fig. 1). Veinlets and offshoots of

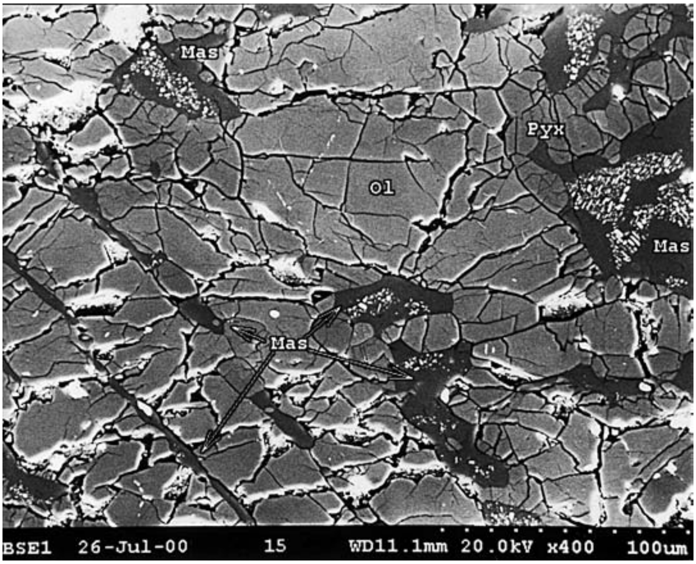


Fig. 4. BSE image showing the occurrence of maskelynite. Note the veinlets, offshoots and melt pockets of maskelynite (Mas) filling fractures and cracks in olivine (Ol) and pyroxene (Pyx). Many maskelynites contain clusters of tiny fragments of chromite (light-grey), olivine and pyroxene (grey). A plagioclase melt pocket (upper right of the image) contains elongated chromite fragments preferentially oriented in two directions.

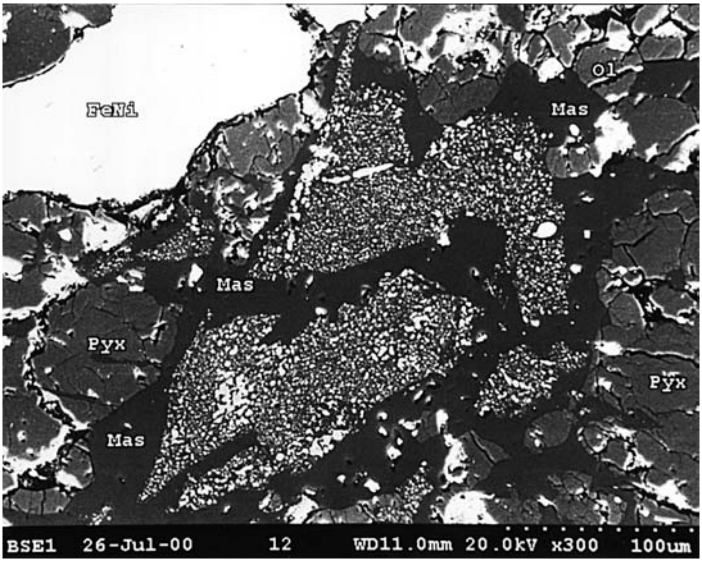


Fig. 5. Clusters of highly granulated chromite fragments with flow-deformed shape in maskelynite (Mas). Pyx – pyroxene, Ol – olivine, FeNi – FeNi metal.

maskelynite are commonly observed (Fig. 4). They were formed through injection of plagioclase melt into fractures or cracks in the neighbouring olivine and pyroxene.

Microprobe analyses (Table 2) show that plagioclase has an oligoclase composition of $(Na_{0.77}K_{0.08}Ca_{0.11}Fe_{0.02})_{0.98}\ Al_{1.01}(Si_{2.91}Al_{0.09})_{3.00}O_8$. The chemical composition of maskelynite,

Table 2. Compositions of plagioclase phases in the Suizhou meteorite (wt %)

| | Plg | Holl | $Mas_1$ | $Mas_2$ | $Mas_{av}$ |
|---|---|---|---|---|---|
| No | 3 | 4 | 3 | 3 | 6 |
| $SiO_2$ | 65.57 | 65.27 | 67.20 | 66.45 | 66.82 |
| $TiO_2$ | 0.04 | 0.04 | 0.06 | 0.05 | 0.05 |
| $Al_2O_3$ | 21.73 | 21.36 | 21.54 | 21.67 | 21.60 |
| FeO | 0.41 | 1.08 | 0.22 | 0.50 | 0.36 |
| MnO | 0.02 | 0.02 | 0.00 | 0.01 | 0.01 |
| MgO | 0.00 | 0.62 | 0.01 | 0.01 | 0.01 |
| CaO | 2.21 | 2.22 | 2.19 | 2.13 | 2.16 |
| $Na_2O$ | 8.87 | 9.14 | 8.35 | 8.94 | 8.64 |
| $K_2O$ | 1.31 | 0.90 | 0.97 | 0.99 | 0.98 |
| $Cr_2O_3$ | 0.03 | 0.01 | 0.03 | 0.01 | 0.01 |
| NiO | 0.00 | 0.00 | 0.01 | 0.02 | 0.01 |
| Totals | 100.38 | 100.16 | 100.76 | 100.77 | 100.65 |
| | | | Number of cations | | |
| Si | 2.84 | 2.91 | 2.93 | 2.90 | 2.92 |
| Ti | 0.00 | 0.00 | 0.00 | 0.00 | 0.00 |
| Al | 1.09 | 1.10 | 1.11 | 1.12 | 1.11 |
| Fe | 0.04 | 0.02 | 0.01 | 0.02 | 0.01 |
| Mn | 0.00 | 0.00 | 0.00 | 0.00 | 0.00 |
| Mg | 0.01 | 0.00 | 0.00 | 0.00 | 0.00 |
| Ca | 0.11 | 0.11 | 0.10 | 0.10 | 0.10 |
| Na | 0.78 | 0.77 | 0.70 | 0.76 | 0.73 |
| K | 0.07 | 0.08 | 0.06 | 0.06 | 0.06 |
| Cr | 0.00 | 0.00 | 0.00 | 0.00 | 0.00 |
| Ni | 0.00 | 0.00 | 0.00 | 0.00 | 0.00 |
| Totals | 4.94 | 4.99 | 4.91 | 4.96 | 4.93 |
| Oxygen | 8 | 8 | 8 | 8 | 8 |

Plg, plagioclase; Holl, hollanite-type $NaAlSi_3O_8$; $Msk_1$, maskelynite;

$Msk_2$, maskelynite containing inclusions; $Msk_{av}$, average for maskelynite;

No, number of analysis.

$(Na_{0.73}K_{0.06}Ca_{0.10}Fe_{0.01})_{0.90}\ Al_{1.03}(Si_{2.92}Al_{0.08})_{3.00}O_8$, is close to that of plagioclase. The very low contents of $Cr_2O_3$, MgO and FeO in maskelynite grains containing chromite and silicate fragments indicate that no exchange of elements has taken place between the host plagioclase melt and the trapped fragments of Cr-, Mg- and Fe-bearing minerals within the plagioclase melt pockets

### 3.4 Chromite fragments in molten plagioclase

Chromite is a common accessory mineral in the Suizhou meteorite. It occurs either in the form of individual grains of irregular shape with grain size < 50 μm, or in the form of inclusions in maskelynite. Both types of chromite are identified by micro-Raman spectroscopic analysis that shows a strong peak at 680 $cm^{-1}$ (Fig. 3d). Fig. 6 shows a shock-deformed chromite grain in contact with pyroxene and maskelynite. This grain displays more abundant irregular and sub-parallel fractures than the neighbouring pyroxene and olivine. Figure 7 demonstrates a cluster of chromite fragments trapped but not homogeneously distributed in a plagioclase melt pocket. The fragments range from 0.4 to 10 μm in sizes. Most of the tiny fragments have rounded shape and smooth surfaces, but some grain outlines and intrafractures of the host chromite grain are still preserved in some larger fragments. This implies that these fragments very likely came from a shock-disaggregated host chromite grain and were subsequently trapped by flowing plagioclase melt. In some cases, chromite grains were shock-granulated into grain size less than 0.4 μm and were then intruded by plagioclase melt, thus forming a unique pattern of clusters of hundreds of tiny rounded or elongated fragments in maskelynite (Fig. 5). We found only one case in which elongated chromite fragments in a maskelynite pocket showed a preferential orientation in two directions (Fig. 4). This phenomenon might be considered at first sight as showing that chromite

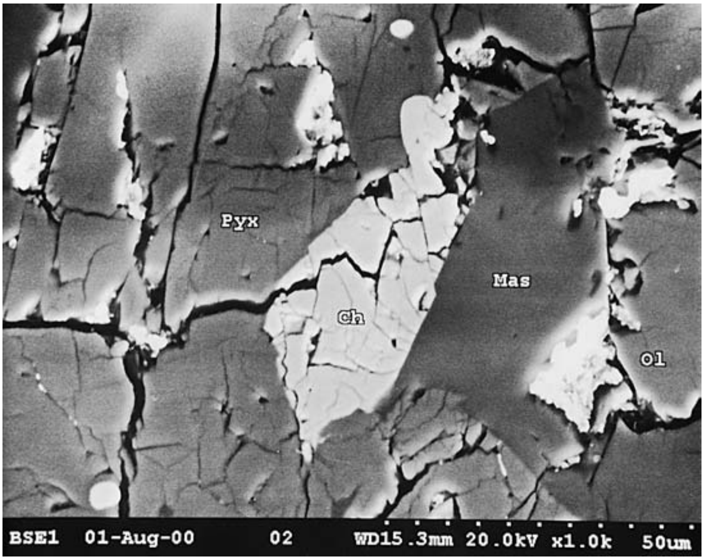


Fig. 6. BSE image showing shock-induced fractures in a chromite (Ch) grain in contact with pyroxene (Pyx) and maskelynite (Mas). Ol – olivine.

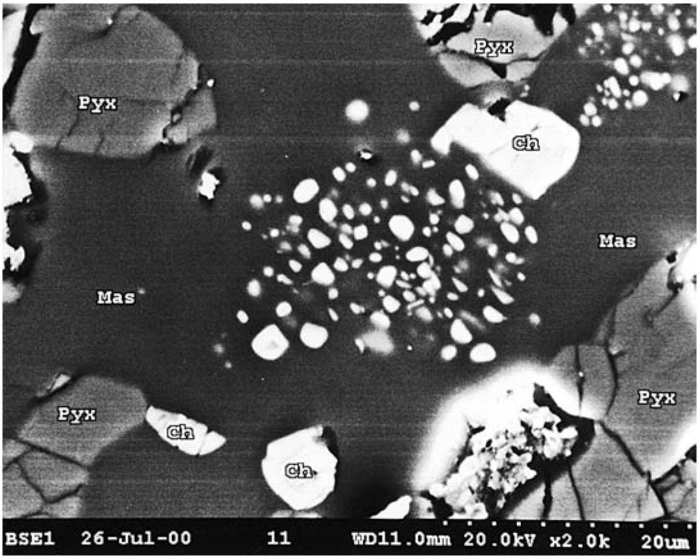


Fig. 7. Chromite (Ch) fragments of different sizes in a maskelynite (Mas) melt pocket. Note the sub-parallel fractures in the larger chromite fragments. Pyx – pyroxene.

slabs recrystallized from the plagioclase melt. However, the much higher melting point of chromite (~ 2000°C) compared with oligoclase and the easy fragmentation of chromite during shock implies that the present orientation of fragments was not produced by melting and recrystallization. Rather, it is due to disaggregation of the host chromite grains along well-developed sub-parallel intrafractures in two sets and subsequent *in-situ* mixing with intruding molten plagioclase.

Our microprobe analyses (Table 3) show that the composition of chromite fragments trapped in plagioclase melt pockets, $(Fe_{0.97}Mg_{0.08}Mn_{0.02})_{1.07}$ $(Cr_{1.49}Al_{0.23}Mg_{0.21}Ti_{0.07})_{2.00}O_4$, is very close to that of chromite grains in the unmelted chondritic rock, $(Fe_{0.94}Mg_{0.05}Mn_{0.02})_{1.01}$ $(Cr_{1.47}Al_{0.24}Mg_{0.16}$

Table 3. Compositions of chromite in the Suizhou meteorite (wt %)

| | Chr 1 | Chr 2 | Chr 3 | Aver. |
|---|---|---|---|---|
| No | 3 | 2 | 2 | |
| $SiO_2$ | 1.77 | 0.37 | 0.07 | 0.74 |
| $TiO_2$ | 2.60 | 2.57 | 2.64 | 2.60 |
| $Al_2O_3$ | 5.78 | 5.49 | 5.72 | 5.66 |
| FeO | 30.77 | 33.25 | 32.41 | 32.14 |
| MnO | 0.55 | 0.57 | 0.53 | 0.55 |
| MgO | 4.14 | 2.46 | 5.72 | 4.12 |
| CaO | 0.04 | 0.05 | 0.04 | 0.04 |
| $Na_2O$ | 0.04 | 0.05 | 0.15 | 0.08 |
| $K_2O$ | 0.01 | 0.05 | 0.00 | 0.02 |
| $Cr_2O_3$ | 53.04 | 53.35 | 55.09 | 53.83 |
| NiO | 0.04 | 0. 16 | 0.02 | 0.07 |
| Totals | 98.81 | 98.41 | 99.21 | 99.85 |

Chr 1, chromite in chondritic rock; Chr 2, chromite in veins; Chr 3, chomite in molten plagioclase; No, number of analysis.

$Ti_{0.07}Si_{0.06})_{2.00}O_4$. The similar contents of $Cr_2O_3$, FeO, $SiO_2$ and $Al_2O_3$ in both types of chromites support our assumption on the origin of the oriented chromite fragments mixed with plagioclase melt.

### 3.5 Weakly-shocked FeNi metal and troilite

Metal and troilite in the Suizhou meteorite occur as single grains of irregular shape, an display no obvious intragranular textures. Raman spectra taken on troilite grains show sharp peaks at 218, 283, 398, 600 and 1292 $cm^{-1}$, indicating that they were weakly deformed by shock. However, some small rounded FeNi metal grains of 0.5 to 5 µm in diameter are observed, but they are not homogeneously distributed in the cracks or intersecting joints of shock-induced planar fractures in olivine and pyroxene (Fig. 8). The chemical composition of these small metal grains was determined using a LINK ISIS 300 X-ray energy dispersive spectrometer attached to SEM. The results show that this type of metal grain has a much lower Fe content (84.58–85.47 wt.%) and higher Ni content (14.53–15.42wt.%) than the large metal grains in the chondritic rock (91.15–94.80 wt.% of Fe and 4.40–6.81 wt.% of Ni) (Wang & Li, 1990). This indicates that the small rounded metal grains might have experienced chemical fractionation during shock-induced melting or evaporation. Therefore, we consider that this type of metal grain was deposited in cracks and fracture joints from nearby shock-induced Ni-rich metal melt or, more likely, from the vapour phase produced from Ni-rich metal during the shock event.

### 3.6 High-pressure phases in shock-melt veins

The thin shock-melt veins in the Suizhou meteorite are mainly composed of a fine-grained

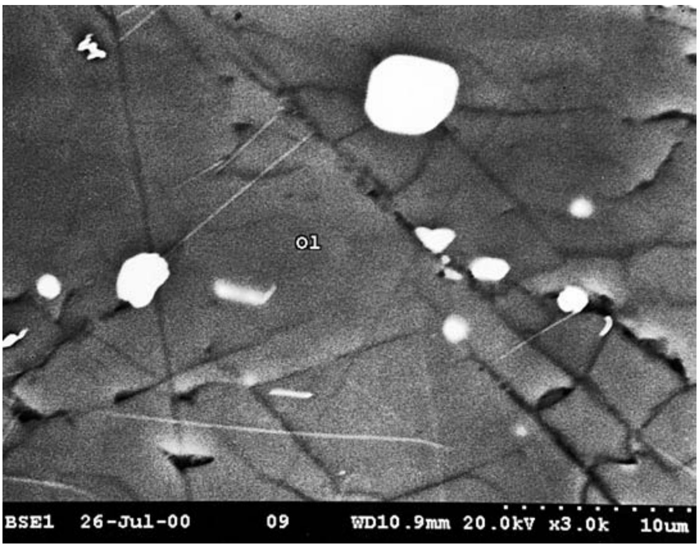


Fig. 8. Small rounded FeNi metal grains (white) deposited in the intersecting joints of shock-induced planar fractures in silicate minerals. Ol – olivine.

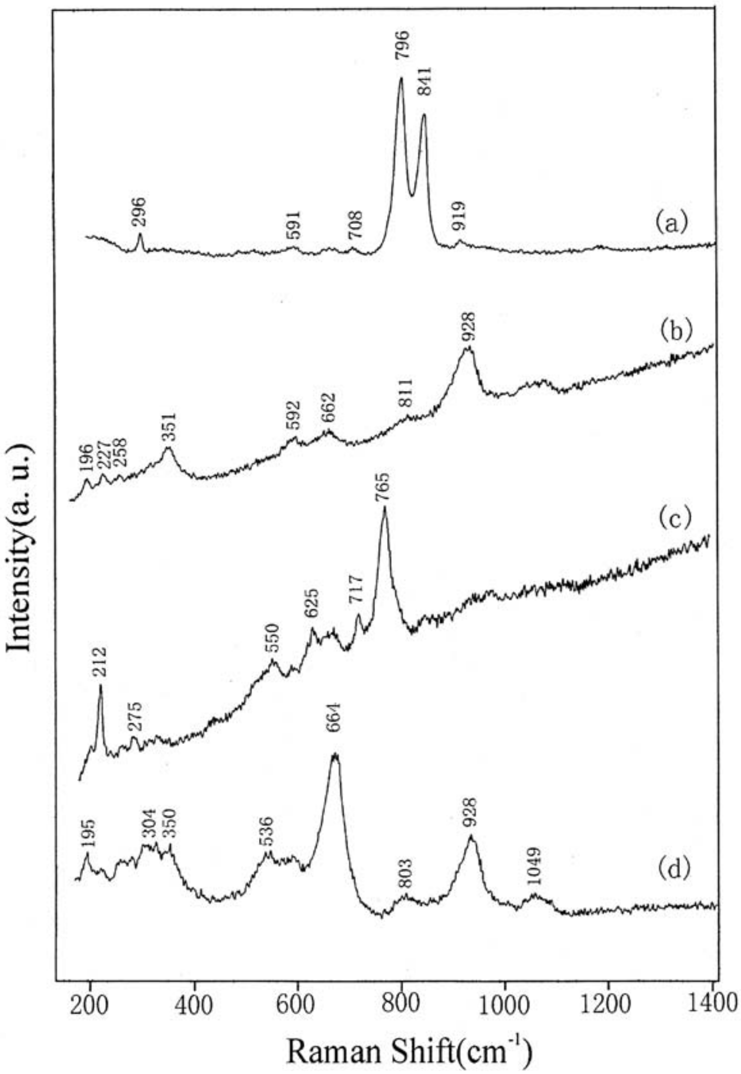


Fig. 9. Raman spectra of high-pressure phases in the Suizhou shock melt veins. (a) ringwoodite, (b) majorite, (c) (Na,Ca)$AlSi_3O_8$-hollandite, and (d) majorite-pyrope$_{ss}$.

matrix that makes up 80~90 volume % of the veins, consisting of majorite-pyrope$_{ss}$ (ss = solid solution), FeNi and FeS eutectic intergrowths. The remaining10~20 volume % of the veins consist of coarse-grained high-pressure phases, including ringwoodite, majorite, and $NaAlSi_3O_8$-hollandite (Xie *et al.*, 2000a, 2000b, 2001).

Ringwoodite, majorite, and $NaAlSi_3O_8$-hollandite in veins have identical compositions as the olivine, low-calcium pyroxene and plagioclase in the host chondritic rock (Tables 1 and 2). On the other hand, the majorite-pyrope$_{ss}$ in the vein matrix is richer in $Al_2O_3$, CaO, $Na_2O$ and $Cr_2O_3$ in comparison with coarse-grained majorite in the same vein and the low-Ca pyroxene in the chondritic rock (Table 1). This suggests that the majorite-pyrope$_{ss}$ was formed by crystallization under high pressure from a shock-induced mixed chondritic melt enriched in these components. Figure 9 shows Raman spectra recorded from four high-pressure phases found in the Suizhou veins. They are characteristic of those obtained from the same high-pressure minerals as indicated by previous investigators (McMillan & Akaogi, 1987; McMillan *et al.*, 1989; Gillet *et al.*, 2000).

## 4. Discussion

### 4.1 First evaluation of shock level of the Suizhou meteorite

Shock effects in olivine and pyroxene in the Suizhou meteorite indicate that these two rock-forming minerals were only shocked to stage 3. Metal and troilite in the meteorite show no obvious intragranular textures. The lack of $^{4}$He and $^{40}$Ar loss from the Suizhou meteorite during the shock event (Wang, 1993) also shows that the shock pressure should be less than about 10 GPa (Stöffler *et al.*, 1991). On the basis of the shock features described above, the Suizhou meteorite can be evaluated as a chondrite shocked to stage 3, which is consistent with the evaluation of previous investigators (Wang & Li, 1990; Wang, 1993). However, in contrast to other shock-vein-bearing L-chondrites, such as Tenham (Langenhost *et al.*, 1995) and Sixiangkou (Chen & El Goresy, 2000), in which the molten plagioclase mainly occurs in domains next to shock veins, almost all plagioclase in the Suizhou unmelted chondritic rock was melted and transformed into maskelynite during the shock event. This implies that the Suizhou meteorite should have a higher shock level than that evaluated from the shock effects in olivine and pyroxene. The presence of shock-melt veins and transition of olivine into ringwoodite indicate that these parts of the meteorite were very strongly shocked to stage 6. Based on the classification and pressure calibration of shock stages defined by Stöffler *et al.* (1991), the whole rock of the Suizhou meteorite could be strongly shocked up to stages S5 with some localized regions (veins) in stage 6. The estimated shock pressure for this meteorite could be in the range of 30~45 GPa.

### 4.2 *P-T* history of plagioclase in the Suizhou meteorite

Shock-wave experiments have shown that feldspar transforms to diaplectic glass at 26-34 GPa, and to melt glass at 42 GPa (Ostertag, 1983). However, the transition process may be accelerated at lower pressures when the temperature is high enough. For instance, the shock-wave experiments of Schmitt (2000) indicate that plagioclase will transform into an amorphous phase at 20-25 GPa if the temperature in the target rock is elevated by about 920 K before the shock, whereas such a transformation at 293 K would take place at 25-30 GPa. It is known that an experimental shock pressure of 30 GPa at the ambient temperature of the chondritic rocks will only produce a temperature rise of less than 350°C (Stöffler *et al.*, 1991). Such a temperature is too low to melt plagioclase although the shock pressure is very high. According to the normal noble gas contents (Wang, 1993) we found no evidence that the Suizhou meteorite was heated to a higher temperature before the shock event. However, the maskelynite occurring in the Suizhou meteorite indicates that the shock-produced temperature must be far higher than 350°C. The investigation on the basaltic meteorite Zagami by Langenhorst & Poirier (2000) revealed that the shock pressure and equilibrium shock temperature might reach 30 GPa and 1000°C, respectively, since all plagioclases in this meteorite were transformed into maskelynite (Langenhorst *et al.*, 1991; McCoy *et al.*, 1992; Chen & El Goresy, 2000). Therefore, we assume that the Suizhou meteorite might be shocked in a pressure range of 25~30 GPa and at a temperature of about 1000°C. According to the scheme of Stöffler *et al.* (1991), this pressure range corresponds to shock stage 4 (15~30 GPa).

It has been emphasized recently by Chen & El Goresy (2000) that phase transitions occurring in many natural impact events could correspond not only to dynamic but more likely kinetic processes as well. The high-pressure pulse in the natural impact events might last for seconds in large impact bodies (Chen *et al.*, 1996; Xie *et al.*, 2001), whereas it takes place only within a time scale of microseconds in shock-wave experiments (Goto & Syono, 1984). This would explain why many shock experiments failed to produce ringwoodite from olivine although the shock pressure is above 56 GPa (Jeanloz *et al.*, 1977). The extended period of higher pressure and temperature regime in the natural impact events might play an important role in the phase transition of minerals in chondrites (Chen *et al.*, 1996; Sharp *et al.*, 1997; Tomioka & Fujino, 1997; Gillet *et al.*, 2000; Xie *et al.*, 2001). We assume that maskelynite could be formed at a shock pressure lower than that in experiments if the duration of high-pressure and temperature regime is long enough. Therefore, we argue that a shock metamprphic regime of 20~25 GPa and ~1000°C in the Suizhou meteorite would be sufficient to transform plagioclase into maskelynite.

### 4.3 *P-T* history of minerals in shock-melt veins of the Suizhou meteorite

The melt veins in the Suizhou meteorite contain abundant high-pressure phases, including coarse-grained ringwoodite, majorite, (Na,Ca) $AlSi_3O_8$-hollandite and fine-grained majorite-pyrope$_{ss}$ which were identified by microprobe and micro-Raman spectroscopic analyses (Table 1 and Fig. 9). According to the experimental data of Katsura & Ito (1989), the formation of ringwoodite with about 80 mol. % of $Mg_2SiO_4$ constrains the pressure to ~18 GPa at 1600°C. The existence of $NaAlSi_3O_8$-hollandite instead of calcium ferrite-type $NaAlSiO_4$ constrains the pressure not higher than 23 GPa at 1000-1200°C (Liu, 1978; Yagi *et al.*, 1994). Experimental results on the Allende meteorite by Agee *et al.* (1995) shows that the assemblage majorite garnet + ringwoodite stabilizes under *P-T* conditions of 18-22 GPa and 1800-1900°C. Therefore, the occurrence of abundant high-pressure phases including ringwoodite, majorite, (Na,Ca)$AlSi_3O_8$-hollandite, and majorite-pyrope$_{ss}$ in the shock melt veins of Suizhou constrains the pressure and temperature to be 18-22 GPa and 1800-1900°C, respectively. This result indicates that minerals in shock-melt veins in the Suizhou meteorite were shocked to pressures similar to those in the unmelted host chondritic rock (20~25 GPa), but to temperatures (~1900°C) much higher than those (~1000°C) in its host rock. Additional heat which raised the temperature of materials in veins might be induced by shear-friction because sharp and straight boundaries between shock veins and surrounding unmelted chondritic rock in the Suizhou meteorite are indicative of strong shearing movement along the veins during the shock event.

We should stress that the estimated pressure range (18-22 GPa) for olivine–ringwoodite transition and other phase transitions in veins in the naturally shocked Suizhou chondrite is much lower than the value (55-90 GPa) evaluated from shock recovery experiments (Stöffler *et al.*, 1991). As we noted previously, this difference may be explained by the longer duration of the high-pressure/high-temperature regime in natural shock events than in shock-loading experiments. But ringwoodite has not been found in shock recovery experiments carried out above 56 GPa (Jeanloz *et al.*, 1977), and it has not been observed in all chondrites with localized melting and recrystallized olivine. Thus Steele & Smith (1978) assumed that special conditions, *e.g.* elevated temperature of the target before shock compression, may be required for the formation of ringwoodite. We propose that the extended duration (a few seconds) of high-pressure and temperature regime in naturally impacted bodies may provide such special conditions. If this is the case, both high pressure and high temperature would be induced in impacted bodies in the first microsecond of a shock compression. This pressure might not be high enough to cause the phase transformation of silicate minerals, but the elevated temperature in impacted bodies would provide favourable conditions for phase transition of minerals when these impacted bodies are still at high pressure. On the other hand, in the case of shock-wave experiments, the condition of elevated temperature may be achieved in small target samples. However, the duration of the high-pressure regime is too short to complete the structural reconstruction of minerals in targets because the target samples decompress within a few microseconds.

### 4.4 Shock history of the Suizhou meteorite

As noted above, the host Suizhou chondritic rock experienced a shock metamorphic regime of up to 20~25 GPa at ~1000°C, whereas the vein material was shocked at up to 18~22 GPa and 1800~1900°C. We take 22 GPa as the upper limit of shock pressure for both the host chondritic rock and the veins. This pressure value is within the pressure range of shock stage 4 (15~30 GPa) (Stöffler *et al.*, 1991).

The presence of small rounded FeNi metal grains deposited from the vapour phase in cracks and fractures joints in the olivine and pyroxene provides additional evidence of the shock temperature produced in the Suizhou meteorite. Experimental vaporization of an L6 chondrite conducted by Gooding & Muenow (1977) showed that the vapour pressure of Fe and Ni is very low (< $10^{-10}$ atm) at < 800°C, but it can reach $10^{-5.5}$ and $10^{-6.5}$ atm at 1200°C. Therefore, these authors indicate that vaporization at < 800°C is not an efficient mechanism for significant transfer of a metal phase unless very long periods of time are available (Gooding & Muenow, 1977). In fact, a temperature of 850-1300°C was estimated for the formation of shock-produced FeNi metal deposited from the vapour phase in the thick-vein-bearing Yanzhuang chondrite (Xie & Chen, 1997). Here, we estimate that the shock temperature in the unmelted host chondritic rock may be about 1000°C. This is in good agreement with the estimation for maskelynite in the chondritic rock.

Based on the shock features of minerals in both unmelted and melted domains, we consider that the Suizhou meteorite was weakly to moderately shock-metamorphosed, and the shock level of the meteorite would be stage 3-4. The shock pressure and temperature are estimated at 22 GPa and 1000°C for the unmelted chondritic rock and 22 GPa and 1900°C for the shock-melt veins.

## 5. Conclusions

The Suizhou L6 chondrite contains weakly shocked olivine, pyroxene, metal and troilite, but almost all plagioclase grains were melted and transformed into maskelynite during the shock event. A few very thin shock-melt veins filled with abundant high-pressure phases are observed in the meteorite. The shock features of this meteorite match the shock stage 3 to 6. The actual shock level of this meteorite was evaluated as stage 3-4. This meteorite experienced a shock pressure and temperature of up to 22 GPa, and ~1000°C, respectively. Locally developed thin shock veins in the meteorite were formed at the same pressure (up to 22 GPa) but at an elevated temperature of about 1900°C. The higher temperature in melt veins than in the unmelted chondritic rock was achieved by localized shear-friction stress. It appears that maskelynite cannot be used as the sole criteria for evaluating the shock stage and estimating the shock pressure in shock-metamorphosed chondrites.

**Acknowledgements:** This study was supported by the National Natural Science Foundation of China under grants 49672098 and 49825106. Special thanks are extended to Pu Yumei of Renishaw Beijing office for her assistance in micro-Raman analyses, and to Han Xiuling for her help in electron microprobe analyses. We are grateful to Dr. H. Leroux for constructive reviews and to M. Canaple and M.S.N. Carpenter for valuable revisions that improved the quality of the manuscript.

## References

Agee, C.B., Li, J., Shannon, M.C., Circone, S. (1995) : Pressure-temperature phase diagram for the Allende meteorite. *J. Geophys. Res.*, **100**, 17725-17740.

Ashworth, J.R. & Barber, D.J. (1975): Electron petrology of shock-deformed olivine in stone meteorites. *Earth Planet. Sci. Lett.*, **27**, 43-54.

—,— (1976): Shock effects in meteoritic pyroxene. *in*: Venable (Editor), "Developments in Electron Microscopy and Analysis", Academic Press, New York, 517-520.

Binns, R.A., Davis, R.J., Reed, S.J.B. (1969): Ringwoodite, natural $(Mg,Fe)_2SiO_4$ spinel in the Tenham meteorite. *Nature*, **221**, 943-944.

Carter, N.L., Raleigh, C.B., DeCarli, P.S. (1968): Deformation of olivine in stone meteorites. *J. Geophys. Res.*, **73**, 5439-5461.

Chen, M. & El Goresy, A. (2000): The nature of maskelynite in shocked meteorites: not diaplectic glass but a glass quenched from shock-induced dense melt at high-pressures. *Earth Planet. Sci. Lett.*, **179**, 489-502.

Chen, M., Sharp, T.G., El Goresy, A., Wopenka, B., Xie, X. (1996): The majorite-pyrope + magnesiowüstite assemblage: constraints on the history of shock veins in chondrites. *Science*, **271**, 1570-1573.

Chen, M., Xie, X., El Goresy, A. (1995): Nonequilibrium solidification and microstructures of metal phases in the shock-induced melt of the Yanzhuang (H6) chondrite. *Meteoritics*, **30**, 28-32.

Dodd, R.T. & Jarosewich, E. (1979): Incipient melting in and shock classification of L-group chondrites. *Earth Planet. Sci. Lett.*, **44**, 335-340.

Fredriksson, K., DeCarli, P., Aaramäe, A. (1963): Shock-induced veins in chondrites. *Space Research*, **III**, 974-983.

Gillet, P., Chen, M., Dubrovinsky, L., El Goresy, A. (2000): Natural $NaAlSi_3O_8$-hollandite in the shocked Sixiangkou meteorite. *Science*, **278**, 1633-1636.

Gooding, J.L. & Muenow, D.W. (1977): Experimental vaporization of the Holbrook chondrite. *Meteoritics*, **12**, 401-408.

Goto, T. & Syono, Y. (1984): Technical aspect of shock compression experiments using the gun method. *in*: I. Sunagawa (Editor), "Materials Science of the Earth's Interior", Terra Scientific Publishing Company, Tokyo, Japan, 605-619.

Jeanloz, R., Ahrens, T.J., Lalley, J.S., Christie, J.M., Heuer, A.H. (1977): Shock produced olivine glass: First observation. *Science*, **197**, 457-459.

Katsura, T. & Ito, E. (1989): The system $Mg_2SiO_4$-$Fe_2SiO_4$ at high-pressures and temperatures: precise determination of stabilities of olivine, modified spinel, and spinel. *J. Geophys. Res.*, **94**, 15663-15670.

Langenhorst, F. & Poirier, J.P. (2000): 'Ecologitic' minerals in a shocked basaltic meteorite. *Earth Planet. Sci. Lett.*, **176**, 259-265.

Langenhorst, F., Stöffler, D., Keil, K. (1991): Shock metamorphism of the Zagami achondrite. *Lunar Planet. Sci.*, **XXII**, 779-780.

Langenhorst, F., Joreau, P., Doukhan, J.C. (1995): Thermal and shock metamorphism of the Tenham chondrite: A TEM examination. *Geochim. Cosmochim. Acta*, **59**, 1835-1845.

Liu, L.G. (1978): High-pressure phase transformations of albite, jadeite and nepheline. *Earth Planet. Sci. Lett.*, **37**, 438-444.

McCoy, T.J., Taylor, G.J., Keil, K. (1992): Zagami: Product of a two-stage magmatic history. *Geochim. Cosmochim. Acta.*, **56**, 3571-3582.

McMillan, P. & Akaogi, M. (1987): The Raman spectra of β-$Mg_2SiO_4$ (modified spinel) and γ-$Mg_2SiO_4$ (spinel). *Am. Mineral.*, **72**, 361-364.

McMillan, P., Akaogi, M., Ohtani, E., Williams, Q., Nieman, R., Sato, R. (1989): Cation disorder in garnets along the $Mg_3Al_2Si_3O_{12}$ – $Mg_4Si_4O_{12}$ join: an infrared, Raman and NMR study. *Phys. Chem. Minerals*, **16**, 428-435.

Ostertag, R. (1983): Shock experiments on feldspar crystals. *J. Geophys. Res.*, **88**, B364-B376.

Schmitt, R.T. (2000): Shock experiments with the H6 chondrite Kernouve: Pressure calibration of microscopic shock effects. *Meteorit. Planet. Sci.*, **35**, 545-560.

Schmitt, R.T. & Stöffler, D. (1995): Experimental data in support of the 1991 shock classification of chondrites (Abstract). *Meteoritics*, **30**, 574-575.

Sharp, T.G., Lingemann, C.M., Dupas, C., Stöffler, D. (1997): Natural occurrence of $MgSiO_3$-ilmenite and evidence for $MgSiO_3$-perovskite in a shocked L chondrite. *Science*, **277**, 352-355.

Steel, I.M. & Smith, J.V. (1978): Coora and Coolamon meteorites: ringwoodite and mineralogical differences. *Lunar Planet. Sci.*, **IX**, 1101-1103.

Stöffler, D., Bischoff, A., Bushward, V., Rubin, A.E. (1988): Shock effects in meteorites. *in:* Kerridge and Matthews (Editors), "Meteorites and the Earth Solar System", Univ. Of Arizona Press, 165-202.

Stöffler, D., Keil, K., Scott, E.R.D. (1991): Shock metamorphism of ordinary chondrites. *Geochim. Cosmochim. Acta*, **55**, 3845-3867.

Tomioka, N. & Fujino, K. (1997): Natural (Mg,Fe)$SiO_3$-ilmenite and -perovskite in the Tenham meteorite. *Science*, **277**, 1084-1086.

Wang, D. (1993): An Introduction to Chinese Meteorites. Science Press, Beijing, China, 101-106.

Wang, R. & Li, Z. (1990): Comprehensive studies on the Suizhou Meteorite. Publishing House of the China University of Geosciences, Wuhan, China, 1-62.

Xie, X. & Chen, M. (1997): Shock-produced vapor-grown crystals in the Yanzhuang meteorite. *Science in China* (D), **40**, 113-119.

Xie, X., Chen, M., Wang, D. (2000a): Natural $NaAlSi_3O_8$-hollandite in the shock melt veins of the Suizhou L6 chondrite. *Antarctic Meteorites*, **XXV**, NIPR, Tokyo, 178-180.

Xie, X., Chen, M., El Goresy, A., Gillet, P. (2000b): Two high-pressure mineral assemblages in shock melt veins of the Suizhou L6 chondrite. *Antarctic Meteorites*, **XXV**, NIPR, Tokyo, 181-183.

Xie, X., Chen, M., Dai, C., El Goresy, A., Gillet, P. (2001): A comparative study of naturally and experimentally shocked chondrites. *Earth Planet. Sci. Lett.*, **187**, 345-356.

Xie, X., Li, Z., Wang, D., Liu, J., Hu, R., Chen, M. (1991): The new meteorite fall of Yanzhuang, a severely shocked H6 chondrite with black molten materials. *Meteoritics*, **26**, 411.

Yagi, A., Suzuki, T., Akaoki, M. (1994): High pressure transitions in the system $KalSi_3O_8$- $NaAlSi_3O_8$. *Phys. Chem. Minerals*, **21**, 12-17.

*Received 23 August 2000*
*Modified version received 5 March 2001*
*Accepted 15 May 2001*